Research Square

Preprints are preliminary reports that have not undergone peer review.
They should not be considered conclusive, used to inform clinical practice,
or referenced by the media as validated information.

Structural Elucidation and Impurity Profiling of Poly (N- Vinylpyrrolidone-co-Maleic Anhydride) Terpolymer Precursors via 1 H- NMR Spectroscopy

Hafsa Ijaz

2021-gcuf-00661@gcuf.edu.pk

Government College University, Faisalabad

Umair Ikram Dar

University of Lahore, Pakistan

Short Report

Keywords:

Posted Date: November 12th, 2026

DOI: https://doi.org/10.21203/rs.3.rs-11295614/v1

License: This work is licensed under a Creative Commons Attribution 4.0 International License.
Read Full License

Additional Declarations: No competing interests reported.

Abstract

Amphiphilic terpolymers with reactive functionalities serve as versatile precursor materials for developing functionalized biomaterial networks. In this study, lauryl/stearyl acrylates, N-vinylpyrrolidone (NVP), and maleic anhydride were employed in radical polymerization to generate two distinct series of hydrophilic oligomers known as the OLPM and OSPM series. High-resolution proton nuclear magnetic resonance (^{1}H-NMR) spectroscopy was utilized as an analytical standard to characterize chemical configurations, map monomer conversion patterns, and quantify trace processing pollutants. Spectroscopic analysis confirmed the effective integration of hydrophilic pyrrolidone heterocyclic rings, hydrophobic acrylate domains, and aliphatic backbones across various monomer feed ratios. The absolute ring-opening hydrolysis of moisture-sensitive maleic anhydride units into active dicarboxylic acid anchors, which are essential for subsequent covalent cross-linking with gelatin amino networks, was unequivocally confirmed by a persistent downfield singlet at δ 12.3 ppm. While minor monomer entrapment and processing solvent residues occurred in mid-tier formulations (OLPM 5 and OSPM 5) due to long-chain alkyl acrylate steric hindrance, optimizing composition dynamics entirely removed these impurities in the highest feed ratio variants. Conclusively, the OLPM 10 and OSPM 10 variants demonstrate refined, impurity-free crosslinking precursors suitable for downstream covalent network formation due to their structural rigidity and high density of crosslinkable dicarboxylic acid groups.

Introduction and Experimental Overview

An essential class of precursor materials for developing advanced biomedical hydrogels are amphiphilic terpolymers with hydrophilic segments and reactive functionalities [1]. With the aim to produce structurally stable networks optimal for cutaneous tissue engineering, two different series of hydrophilic oligomers known as the OLPM and OSPM series were produced by radical polymerization utilizing lauryl/stearyl acrylates, *N*-vinylpyrrolidone (NVP), and maleic anhydride [2]. Briefly, at 70 °C free-radical polymerization was carried out in 1,4-dioxane for 6 h utilizing azobisisobutyronitrile (AIBN) as the thermal initiator, followed by repeated precipitation in cold diethyl ether and drying under vacuum at 40 °C to yield the purified oligomeric precursors. Considering that leftover unreacted vinyl monomers induce localized cytotoxicity and acute inflammation in open cutaneous applications, precise structure elucidation, monomer incorporation ratios, and chemical purity are vital [3]. High-resolution proton nuclear magnetic resonance (^{1}H-NMR) spectroscopy was employed as a basic analytical benchmark before gelatin matrix crosslinking to assure strict quality control and map the critical ring-opening hydrolysis of moisture-sensitive maleic anhydride units into reactive dicarboxylic acid anchors [4]. For spectroscopic characterization, approximately 10-15 mg of each produced oligomeric variant (including OLPM 2.5, 5, 10 and OSPM 2.5, 5, 10 matrices) was entirely dissolved in 0.6 mL of high-purity dimethyl sulfoxide-d6 (DMSO-d_6). All ^{1}H-NMR experiments were cataloged at room temperature on a Bruker spectrometer operating at a standard resonance frequency (500 MHz) [5]. Chemical shifts (δ) were recorded in parts per million (ppm) and scrupulously calibrated relative to an internal tetramethylsilane (TMS) reference standard set at δ = 0.0ppm. Raw free induction decays (FIDs) were processed utilizing

Bruker TopSpin software, introducing manual phasing, intensive baseline flattening adjustments to precisely resolve crowded aliphatic envelopes, and exponential multiplication with a line-broadening factor of 0.3 Hz to optimize signal-to-noise ratios [6]. Quantitative integrations of specific structural markers particularly the terminal methyl ends (δ 0.85–0.88 ppm), pyrrolidone ring protons (δ 1.9–3.5 ppm), and the downfield hydrolyzed carboxylic acid singlets (δ 12.3 ppm) were implemented to map monomer conversion profiles and assess trace solvent or purification processing impurities [7].

Results & Discussion

^{1}H-NMR spectroscopy was employed in both the OLPM and OSPM series to examine the chemical structure of the synthesized hydrophilic oligomers before gelatin crosslinking. The spectra indicated that the structural domains essential for hydrogel network development were effectively integrated.

All of the characteristic peaks for the hydrophobic tail fractions of the acrylate and the highly hydrophilic heterocyclic ring environments are successfully represented in the spectrum for the lowest feed ratio formulation, OLPM 2.5 (Fig. 1a). The methylene spacer and ester linkage areas significantly broaden as the monomer ratios shift in OLPM 5 (Fig. 1b), demonstrating the integrated existence of the longer-chain segments. Minor residual processing and monomer contaminants from late-stage synthesis purification were also identified in this sample. The signals corresponding to the hydrophilic pyrrolidone ring protons enhanced in relative strength when the concentration of modifying monomers was raised in OLPM 10 (Fig. 1c). The methine protons that contribute to the primary polymer spine and the nitrogen-adjacent ring protons were observed to substantially overlap in space at the same time. The formation of the deep downfield singlet at δ 12.3 ppm indicated that the ring-opening hydrolysis of the maleic anhydride rings was consistently effective in all three OLPM forms. The crucial free carboxylic acid (-COOH) functionalities essential for further crosslinking with the amino groups of the gelatin matrix are formed by this transformation into dicarboxylic acid units.

A corresponding structural development toward a functionalized hydrophilic precursor was illustrated by the OSPM series. The projected overlapping configuration of the NVP ring segments with the polymerized maleic backbone was observed in the OSPM 2.5 spectrum (Fig. 2a). As the formulation shifted to OSPM 5, the quantitative integration of the downfield carboxylic acid singlet generated a relative value of 4.23, which steadily declined to 2.86 (Fig. 2b). Trace indications associated with residual processing chloroform and mild monomer unsaturation were observed in both mid-tier formulations. Conversely, the OSPM 10 spectrum (Fig. 2c), which was calibrated using an internal TMS reference, had a very distinct baseline. The saturated backbone of the oligomer was clearly distinguished because this sample was processed utilizing a pure DMSO-d6 system. The adjacent NVP ring fractions provided for the full resolution of the real backbone methylene and methine connections. The entire absence of alkenic impurities in this final sample reveals a highly pure, effectively hydrolyzed oligomeric matrix employed in hydrogel formulation, which is crucial for downstream biomedical applications requiring high chemical purity.

The spectroscopic profiles of the OLPM and OSPM series confirm the effective integration of functionalized hydrophilic oligomeric precursors, representing how systematic monomer variations influence precursor composition prior to network crosslinking. The continuous saturation of vinyl monomers into a covalent network is verified by the wide aliphatic backbone envelopes. Steric hindrance significantly impacts the propagation kinetics in random radical terpolymerizations utilizing long-chain alkyl acrylates[8]. The preservation of small unreacted vinyl fragments and the entrapment of processing solvent in the dense cores of mid-tier formulations (OLPM 5 and OSPM 5), where extensive stearyl chains restrict local macromolecular mobility and hinder solvent removal, are mediated by this steric shielding [9]. Contrarily, optimizing the hydrophilic and carboxylic constituents in OLPM 10 and OSPM 10 shifts the equilibrium to eradicate residual unsaturation and build pure matrices by balancing reactivity ratios.

Regulating the hydrogel swelling kinetics and wound exudate absorption demands adjustment of the hydrophobic-hydrophilic balance within the crosslinking precursor [10]. When *N*-vinylpyrrolidone (NVP) is incorporated, hydrophilic pyrrolidone heterocyclic rings emerge as excellent water-binding coordinates [11], scaling up dynamically across the formulations. Additionally, a highly confined, stiff local conformation is demonstrated by the spatial overlap between the methine protons in the polymer spine and the nitrogen-adjacent ring protons. This localized structural rigidity gives a stable macromolecular framework that can influence the mechanical stability of resulting polymer networks [12].

The ring-opening hydrolysis of maleic anhydride fractions into dicarboxylic acid units, which is marked by a substantial downfield carboxylic acid singlet in all variations, is the most important chemical change that has been validated. Moisture-sensitive anhydrides are converted into stable, incredibly reactive free carboxylic acid (-COOH) functionalities in this phase [13]. Changes in this peak's integration reveal that water accessibility to the anhydride ring during hydrolysis is regulated by the local steric environment. These released carboxyl groups are vital for hydrogel production because they serve as chemical anchors essential to heat or carbodiimide-mediated (EDC/NHS) crosslinking with the free ε-amino groups of lysine residues along the gelatin backbone [14]. Because unreacted acrylic or vinyl monomers pose known biocompatibility risks [15], quantitative spectroscopic monitoring of residual unsaturation provides an essential quality-control parameter before clinical translation [16].

The ideal, impurity-free baseline achieved for OSPM 10 indicates that a pure, effectively hydrolyzed oligomeric matrix can be obtained, even while trace monomer impurities in mid-tier formulations emphasize the demand for strict vacuum extraction for bulkier terpolymers. The highest feed-ratio formulations act as optimal candidates for hydrogel fabrication owing to their high chemical purity, water-binding pyrrolidone content, and abundant crosslinkable carboxylic acid sites [4].

Conclusion

The synthesized OLPM and OSPM amphiphilic oligomeric series' structural configurations, monomer insertion kinetics, and composition profiles were successfully verified by high-resolution ^{1}H-NMR

spectroscopy. By precisely tracing the complete ring-opening hydrolysis of moisture-sensitive maleic anhydride rings into active dicarboxylic acid units across all configurations, spectroscopic profiling produced an essential chemical baseline for subsequent covalent cross-linking with gelatin amino networks. Furthermore, purity tracking identified critical kinetic discrepancies, revealing that while long-chain alkyl acrylate steric hindrance leads to trace monomer entrapment and processing solvent residues within the mid-tier matrices (OLPM 5 and OSPM 5), optimizing the precursor compositions entirely eliminates these impurities in the highest feed ratio formulations. Ultimately, due to its highly pure baseline, high density of crosslinkable dicarboxylic acid groups, and water-binding pyrrolidone rings the optimized OSPM 10 variant represents a structurally refined crosslinking precursor for hydrogel synthesis.

Declarations

Conflict of interest

The authors declare no conflict of interest, financial or otherwise.

Funding

No funds, grants, or other support was received.

Author Contribution

H.I. conceived and designed the project workflow, managed the retrieval and repository organization of raw nuclear magnetic resonance (NMR) data files, performed all digital processing, phase-correction, and baseline optimization tasks within the Bruker TopSpin software environment, generated the final multi-panel figures, and wrote the main manuscript text. U.I.D. assisted content and structural assignment validation. All authors reviewed, edited, and approved the final version of the manuscript.

Acknowledgements

Declared none.

Data Availability

All research data generated or analyzed during this study including the fully processed 1H-NMR baselines, structural integrations, and peak assignments are included in this published brief report and

its accompanying Supplementary Information files. Any additional data if required are available from the corresponding author upon reasonable request.

References

1. Lin C, Gitsov I (2010) Synthesis and Physical Properties of Reactive Amphiphilic Hydrogels Based on Poly(*p*-chloromethylstyrene) and Poly(ethylene glycol): Effects of Composition and Molecular Architecture. Macromolecules 43(7):3256–3267. https://doi.org/10.1021/ma9026564
2. Xing J, Deng L et al (2009) Amphiphilic poly{[α-maleic anhydride-ω-methoxy-poly(ethylene glycol)]-co-(ethyl cyanoacrylate)} graft copolymer nanoparticles as carriers for transdermal drug delivery. Int J Nanomed. https://doi.org/10.2147/ijn.s7814
3. Kirf D, Higginbotham L (2010) Cyto- and genotoxicological assessment and functional characterization of N-vinyl-2-pyrrolidone-acrylic acid-based copolymeric hydrogels with potential for future use in wound healing applications. Biomed Mater. https://doi.org/10.1088/1748-6041/5/3/035002
4. Loth T, Hötzel R et al (2014) Gelatin-Based Biomaterial Engineering with Anhydride-Containing Oligomeric Cross-Linkers. Biomacromolecules 15(6). https://doi.org/10.1021/bm500241y
5. Bagheri M, Bresseleers J et al (2018) Effect of Formulation and Processing Parameters on the Size of mPEG-*b*-p(HPMA-Bz) Polymeric Micelles. Langmuir 34(50). https://doi.org/10.1021/acs.langmuir.8b03576
6. Wang B, Maldonado-Devincci M (2021) Evaluating line-broadening factors on a reference spectrum as a bucketing method for NMR based metabolomics. Anal Biochem. https://doi.org/10.1016/j.ab.2020.113872
7. Verduzco LE, García-Pérez L (2021) Bioconjugation of papain with poly(N-vinylpyrrolidone): NMR characterization and study of its enzymatic activity. Can J Chem 99. https://doi.org/10.1139/cjc-2020-0181
8. el Shazly R, Kamal S (2020) R, The behavior of some terpolymers as lubricating oil additives. Appl petrochem res
9. Gao C, Yan Y (2004) Hyperbranched polymers: from synthesis to applications. Prog Polym Sci. https://doi.org/10.1016/j.progpolymsci.2003.12.002
10. Rahman M, Teimouri S et al (2025) Strategies for Regulating the Release Kinetics of Bioactive Compounds from Biopolymeric Hydrogels. Gels 11(12). https://doi.org/10.3390/gels11120986
11. Teodorescu M, Bercea M (2015) Poly(vinylpyrrolidone) – A Versatile Polymer for Biomedical and Beyond Medical Applications. Polym -Plast Technol Eng. https://doi.org/10.1080/03602559.2014.979506
12. Zhang Z, Wang Q et al (2012) Fabrication of novel nanoporous array anodic alumina solid-phase microextraction fiber coating and its potential application for headspace sampling of biological volatile organic compounds. Anal Chim Acta. https://doi.org/10.1016/j.aca.2012.03.033

13. Italo de Oliveira Brito M, De Jesus Hiller N et al (2025) Maleic Anhydride (CAS: 108-31-6): A Valuable Tool for both Industry and Scientific Research. Rev Virtual Quim. https://doi.org/10.21577/1984-6835.20250012
14. Kuijpers A, Engbers G et al (2000) Cross-linking and characterisation of gelatin matrices for biomedical application. J Biomater Sci Polym Ed. https://doi.org/10.1163/156856200743670
15. Yoshii E (1997) Cytotoxic effects of acrylates and methacrylates: relationships of monomer structures and cytotoxicity. J Biomed Mater Res. https://doi.org/10.1002/(sici)1097-4636(19971215)37:4%3C517::aid-jbm10%3E3.0.co;2-5
16. Boateng S, Matthews JH (2008) Wound healing dressings and drug delivery systems: a review. J Pharm Sci. https://doi.org/10.1002/jps.21210

Figures

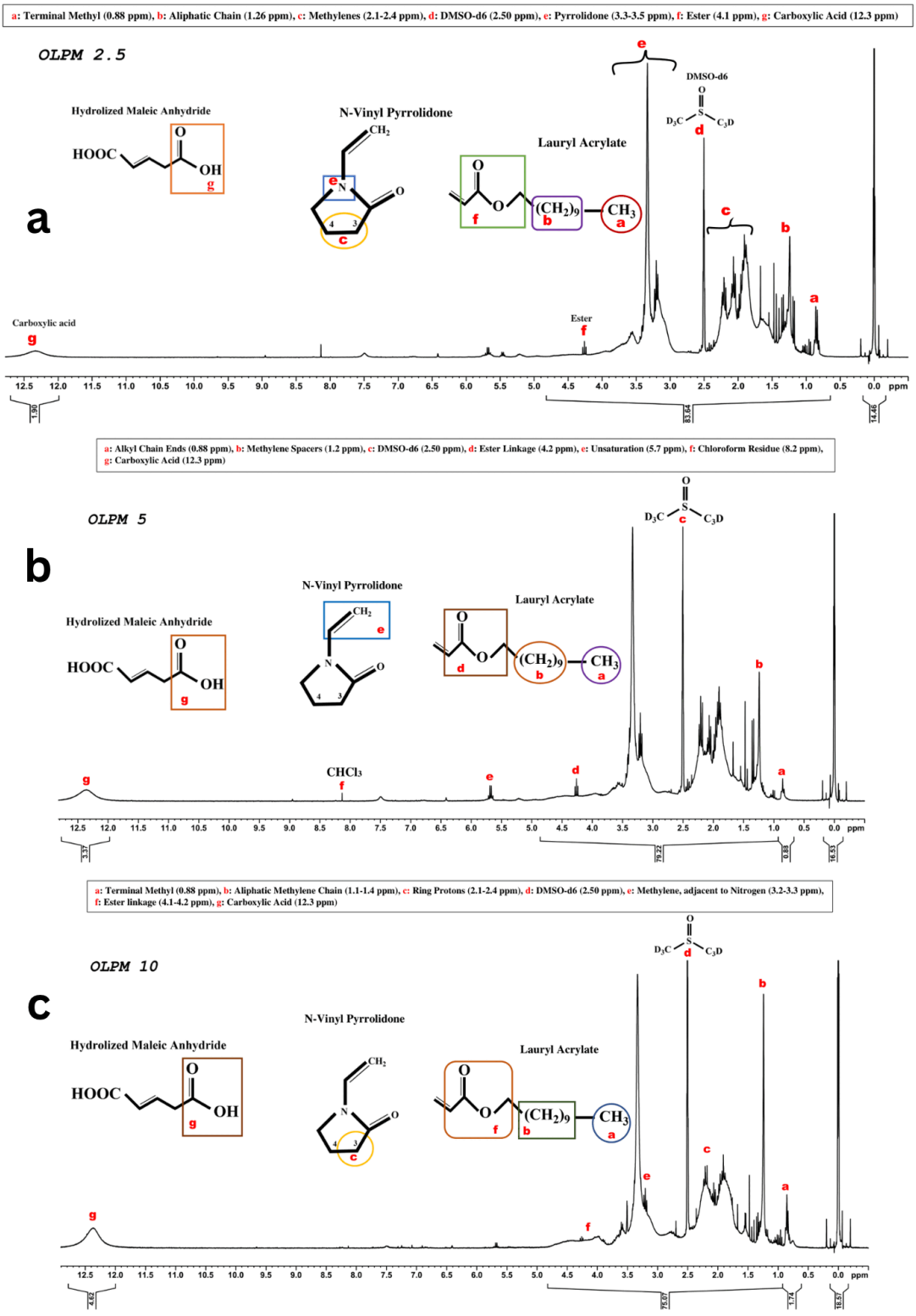


Figure 1

Multi-panel ^{1}H-NMR spectroscopic characterization of the synthesized OLPM copolymer series across varying monomer feed ratios. **a** The ^{1}H-NMR spectrum of the lowest feed ratio formulation (OLPM 2.5) demonstrates a baseline composition where successful synthesis is confirmed by distinct lauryl acrylate terminal methyl (δ 0.88 ppm) and long aliphatic methylene chain (δ 1.26 ppm) indicators, alongside its characteristic ester linkage (-O-CH2-) at δ 4.1 ppm. Successful incorporation of N-vinylpyrrolidone is

verified by isolated ring methylene signals (δ 2.1-2.4 ppm) and the downfield -N-CH2- ring environment (δ 3.3-3.5 ppm). **b** In the mid-tier formulation (OLPM 5), the spectrum reflects a shift in structural development characterized by significant broadening of the methylene spacer and ester linkage resonances (δ 3.4-4.2 ppm) representing the integration of longer-chain stearyl segments. This panel explicitly captures late-stage purification limits, where trace monomer unsaturation at δ 5.7 ppm and a residual chloroform processing solvent signal at δ 8.2 ppm appear due to steric entrapment. **c** The terminal formulation spectrum (OLPM 10) showcases a substantial increase in modifying monomer density, marked by enhanced relative signal intensities for the hydrophilic pyrrolidone rings. At this concentration, steric crowding leads to an increased spatial overlap between the primary polymer backbone methine protons and the nitrogen-adjacent ring protons (δ 3.2-3.3 ppm). Across all three panels (**a-c**), a consistent downfield singlet at δ 12.3 ppm confirms successful ring-opening hydrolysis of moisture-sensitive maleic anhydride units into reactive dicarboxylic acid crosslinking anchors, while residual DMSO-d6 solvent remains stabilized at δ 2.50 ppm.

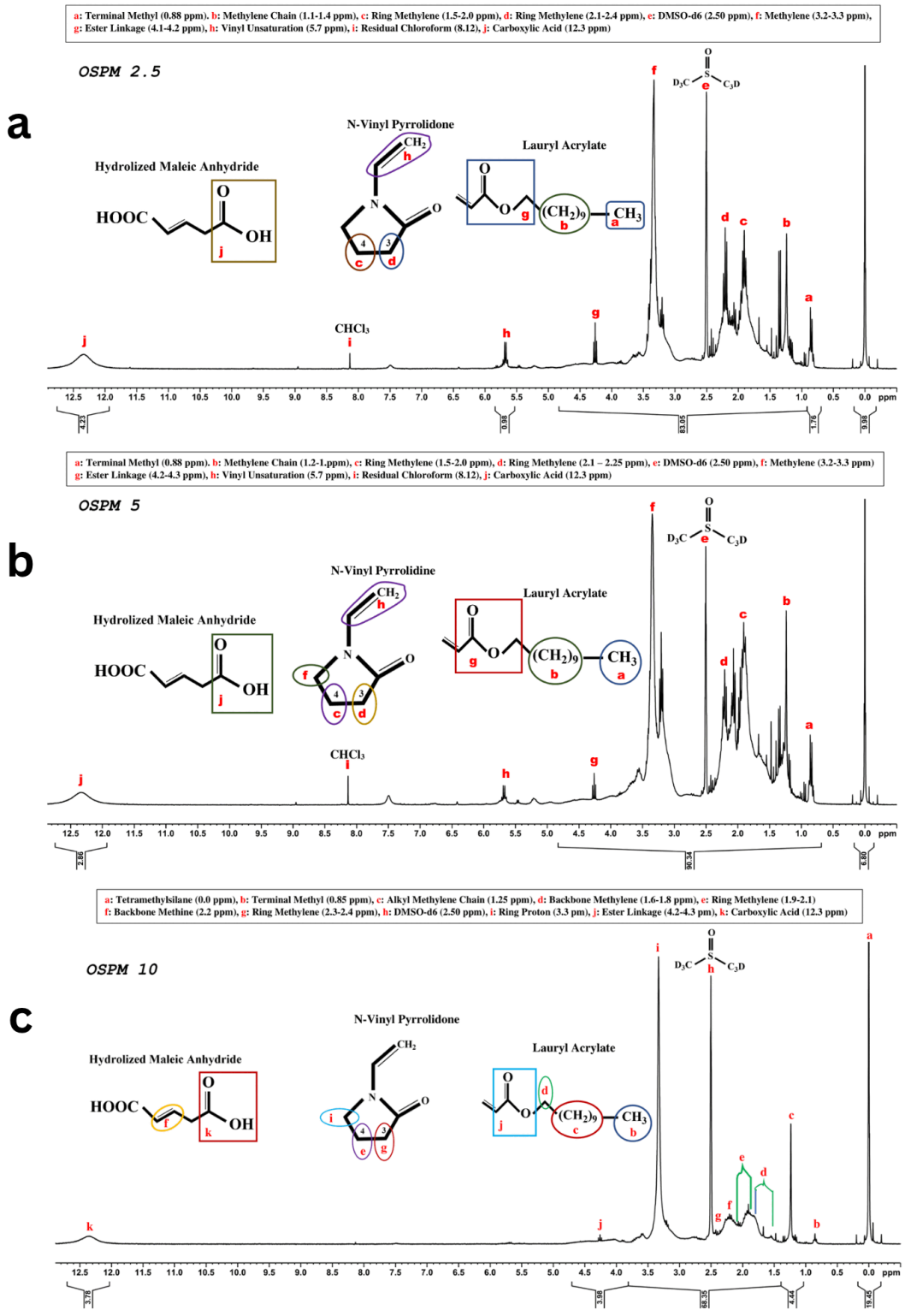


Figure 2

Multi-panel ^{1}H-NMR spectroscopic characterization of the synthesized OSPM terpolymer precursor series under varying monomer ratios. **a** The 1H-NMR spectrum of the lowest feed ratio formulation (OSPM 2.5) displays a baseline confirming successful synthesis via characteristic lauryl and stearyl acrylate terminal methyl (δ 0.88 ppm) and long methylene chain (δ 1.1-1.4 ppm) indicators, alongside the ester linkage (-O-CH2-) at δ 4.1-4.2 ppm. N-vinylpyrrolidone incorporation is verified by ring

methylene environments (δ 2.1-2.4 ppm), which overlap closely with the methine protons of the polymerized maleic anhydride spine (δ 3.2-3.3 ppm). This panel tracks an initial pronounced carboxylic acid resonance at δ 12.3 ppm with a quantitative integration value of 4.23, while noting trace monomer unsaturation (δ 5.7 ppm) and residual chloroform solvent (δ 8.12 ppm**). b** In the mid-tier formulation (OSPM 5), the spectrum preserves an identical macro-structural environment but exhibits a distinct kinetic shift, marked by a contraction of the hydrolyzed carboxylic acid singlet integration at δ 12.3 ppm down to 2.86. Persistent minor monomer residuals (δ 5.7 ppm) and trapped chloroform processing impurities (δ 8.12 ppm) remain visible due to localized long-chain steric shielding. **c** The terminal formulation spectrum (OSPM 10) showcases a highly refined, impurity-free baseline calibrated directly against an internal tetramethylsilane (TMS) standard at δ 0.0 ppm. The spectrum isolates pristine structural indicators: backbone methylene segments (δ 1.6-1.8 ppm), backbone methines (δ 2.2), and resolved pyrrolidone ring environments (δ 1.9-2.1 ppm, δ 2.3-2.4 ppm, and δ 3.3 ppm). Across all three panels (**a-c**), the continuous presence of the downfield carboxylic acid singlet at δ 12.3 ppm documents the absolute ring-opening hydrolysis of maleic anhydride units into active dicarboxylic acid anchors, while residual DMSO-d6 solvent remains anchored at δ 2.50 ppm.

Supplementary Files

This is a list of supplementary files associated with this preprint. Click to download.

- OLPM2.5.tiff
- OLPM5.tiff
- OLPM10.tiff